

PAPER • OPEN ACCESS

## The investigation of strength and plasticity mechanism of low-temperature annealed ultrafine grained stainless steel

To cite this article: Q H Pang *et al* 2018 *IOP Conf. Ser.: Mater. Sci. Eng.* **372** 012038

View the [article online](#) for updates and enhancements.

You may also like

- [Effect of hot stamping and quenching & partitioning process on microstructure and mechanical properties of ultra-high strength steel](#)  
Cainian Jing, Daomin Ye, Jingrui Zhao et al.
- [Effects of cryogenic treatment on mechanical properties and crystal orientation of 0.25C-0.80Si-1.6Mn steel with extraordinary strength-toughness](#)  
Yongli Chen, Yuhua Li, Xuejiao Zhou et al.
- [CO<sub>2</sub> corrosion behavior of high-strength martensitic steel for marine riser exposed to CO<sub>2</sub>-saturated salt solution](#)  
Dazheng Zhang, Xiuhua Gao, Weijuan Li et al.



**ECS**  
The  
Electrochemical  
Society  
Advancing solid state &  
electrochemical science & technology

**DISCOVER**  
how sustainability  
intersects with  
electrochemistry & solid  
state science research

# The investigation of strength and plasticity mechanism of low-temperature annealed ultrafine grained stainless steel

Q H Pang<sup>1,2</sup>, W J Li<sup>1,2,3</sup>, M Y Cai<sup>1,2</sup>, H Qi<sup>1,2</sup>, C C Zhang<sup>1,2</sup> and J N Wu<sup>1,2</sup>

<sup>1</sup>School of Materials and Metallurgy, University of Science and Technology Liaoning, Anshan Liaoning, 114051, China

<sup>2</sup>State Key Laboratory of Metal Material for Marine Equipment and Application, Anshan Liaoning, 114009, China

E-mail: liweijuan826@163.com

**Abstract.** The properties of steel material can be greatly improved when its grain size becomes finer, so grain refinement is the most commonly used to improve the strength, ductility and impact on the toughness of steel at the same time. Compared to ordinary fine-grained steel, the average grain size of ultra-fine grained steel is less than 2  $\mu\text{m}$  and it has different strength and plasticity mechanism. In this paper, effect of low-temperature annealing on the microstructure and properties of ultra-fine grained stainless steel in internal friction was studied by utilizing transmission electron microscope (TEM) and universal tensile testing machine. At the same time, the strength and plasticity mechanism of ultra-fine grained stainless steel was revealed by internal friction experiments. The results show that with the increase of annealing time and annealing temperature, both the tensile strength and yield strength decreases, while the elongation increases continuously. The mechanical properties of tested steel are more sensitive to the temperature. In the internal friction curve of tested steel, the peak of  $P_1$  which result from the interaction between solid solution atoms and dislocations increases first and then decreases, while the peak of  $P_2$  which result from the interaction between dislocation and carbide precipitates decreases first and then increases. The peak of  $P_3$  which result from the structure, area and movement of grain boundary decreases continuously. The strength and plasticity mechanism of tested steel at room temperature is the result of interaction between the grain boundary and dislocation.

## 1. Introduction

When the average grain size of material is between 100 nm and 2  $\mu\text{m}$ , we ordinarily call it ultrafine-grained material. Due to its high fracture strength, high specific strength, high specific stiffness and excellent wear resistance, it has been more and more widely applied in transportation, aerospace, electrical and electronic fields [1-3]. The methods of ECAP (equal channel angular pressing) [4], HPT (high pressure torsion) [5], electrodeposition [6], cyclic extrusion-upsetting [7] and powder metallurgy [8] etc can prepare ultrafine grained material, but these methods are difficult to produce ultrafine-grained materials as components over 30 cm diameter or length. At present, the forging (or rolling) with large deformation and then recrystallization annealing is used to achieve large size ultrafine grained material [1,9,10], so the regulation of its thermal stability is the key factor to the success preparation of ultrafine-grained material. Numerous studies [11-14] have shown that the key influence factors of thermal stability in ultrafine grained material are the heating temperature and heating time.



The heating temperature directly affects the activation energy of grain boundary diffusion. When the ambient temperature exceeds a certain temperature (critical temperature), the grain size will increase exponentially with the increase of temperature. On the other hand, the heating time affects the degree of grain growth. Fereshteh E [15] prepared nanoscale nickel base alloy with grain sizes of 11 nm, 59 nm and 278 nm at 250°C, 400°C and 500°C annealing 90 min, respectively.

Compared with ordinary steel, the strength and hardness of ultrafine-grained steel increased significantly, but its elongation decreased significantly. Even for steel with good plasticity under the conventional grain size, its elongation at break was less than 5% [6,16]. For instance, the grain size of ferrite in carbon steel with 0.55% carbon content was 1.7  $\mu\text{m}$ ~30 nm. Its strength increased gradually with the grain size refined, but the plasticity decreases obviously [17]. For IF steel whose the average grain size is in 12  $\mu\text{m}$ ~0.45  $\mu\text{m}$ , the stress-strain curve changed from continuous yielding to discontinuous yielding with the grain refined. When the grain size was less than 1  $\mu\text{m}$ , the elongation after fracture decreased suddenly [18]. When the average grain size of ferrite in medium carbon steel was less than 150 nm, there was no necking phenomenon before fracture, and the fracture would suddenly occur [19]. Therefore, the research of strength and plasticity mechanism in ultrafine-grained material is a very important research content, and further investigation is required.

The change of point, line and surface defect in the material inside will directly determine the plastic deformation behavior during uniaxial tensile test. In this paper, the effect of different annealing processes on microstructure, mechanical properties and internal friction of ultrafine-grained stainless steel was studied. According to the spectrum of internal friction, the relationship between microcosmic state (such as solid solution atoms, dislocation and grain boundary) and mechanical properties was analyzed. Meanwhile, the strength and plasticity mechanism of ultrafine-grained stainless steel was revealed.

## 2. Experimental work

Experimental materials are ultrafine-grained cold rolled stainless steel provided by a factory, with its chemical composition as shown table 1. Samples were heated to 300°C, 350°C, 400°C and 500°C, and held 20 min, 30 min, 60 min and 120 min respectively, to anneal. Finally, the samples were cooled down slowly to room temperature in an insulated blanket.

**Table 1.** Chemical composition of tested steels (wt%).

No.	C	Si	Mn	P	S	Ni	Cr	Mo	V	Nb
Tested steel	0.055	0.4	1.63	$\leq 0.035$	$\leq 0.03$	8.45	17.3	0.12	0.08	0.04
316L	$\leq 0.03$	$\leq 1.00$	$\leq 2.00$	$\leq 0.035$	$\leq 0.03$	10.0-14.0	16.0-18.0	2.0-3.0	—	—

The samples for transmission electron microscope were cut from the annealed sample and grinded to 50  $\mu\text{m}$  thick foils, and then twin-jet electropolished with 5% perchloric acid alcohol solution (volume fraction) at 35~45 V. The microstructures were analyzed using JEM-2100 transmission electron microscope (TEM). The tensile load was applied with a constant strain rate of  $5 \times 10^{-3}$  m/sec. From the engineering stress strain curve, the yield strength was calculated by 0.02% offset method.

Internal friction experiments were performed in MFP-1000 multifunctional internal friction instrument. The internal friction-temperature spectrum was measured by the free attenuation method, and free attenuation frequency was 2.78 Hz. The actual friction curve can be obtained by the deduction of background internal friction [20], and the relaxation activation energy of actual internal friction peak are measured according to equation (1).

$$H = RT_m \ln(K_B T_m / hf_m) + T_m \Delta S \quad (1)$$

Where  $T_m$  means peak temperature,  $f_m$  means peak frequency,  $R$  means the gas constant,  $K_B$  means the boltzmann constant,  $h$  means the Panck constant,  $\Delta S$  means entropy change whose value is  $1.1 \times 10^{-4}$  Ev/k.

### 3. Experimental results

#### 3.1. Mechanical properties

Figure 1 shows the stress-strain curve of ultrafine-grained stainless steel annealed at 400°C and soaked different time. Initial tested steel has the maximum tensile strength and yield strength, and the minimum elongation after fracture as illustrated in figure 1(a). Their values are respectively 1403 MPa, 893 MPa and 11%. With the extension of tempering time, the strength and yield strength of tested steels both decrease, and the decrease degree of tensile strength is greater than that of yield strength. While the elongation after fracture steeply increases at the beginning, and then the raise of them becomes progressively slower as illustrated in figure 1(b).

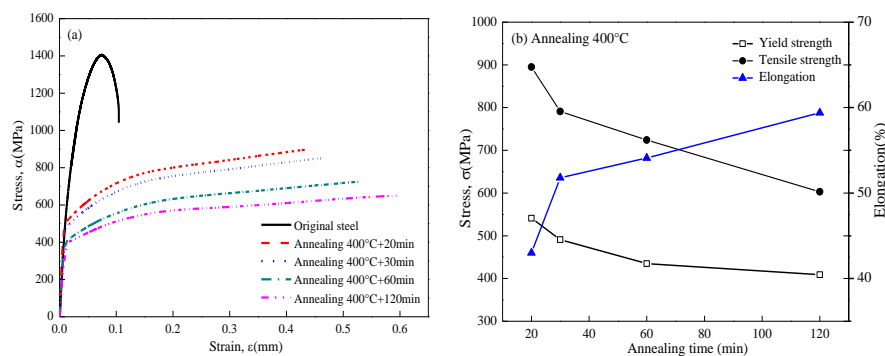


Figure 1. Tensile stress-strain curves of tested steels with different annealing time.

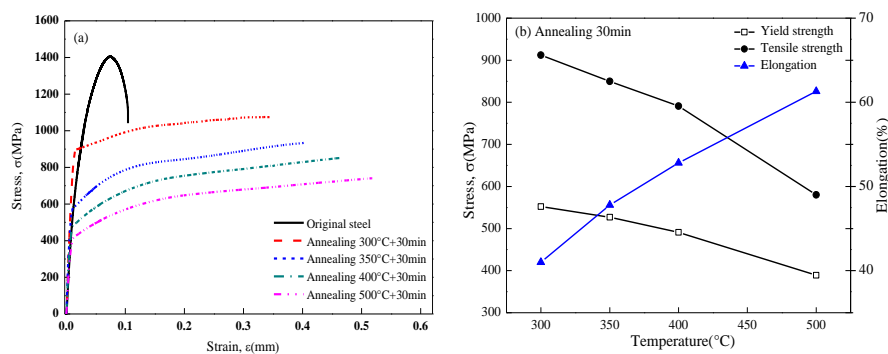
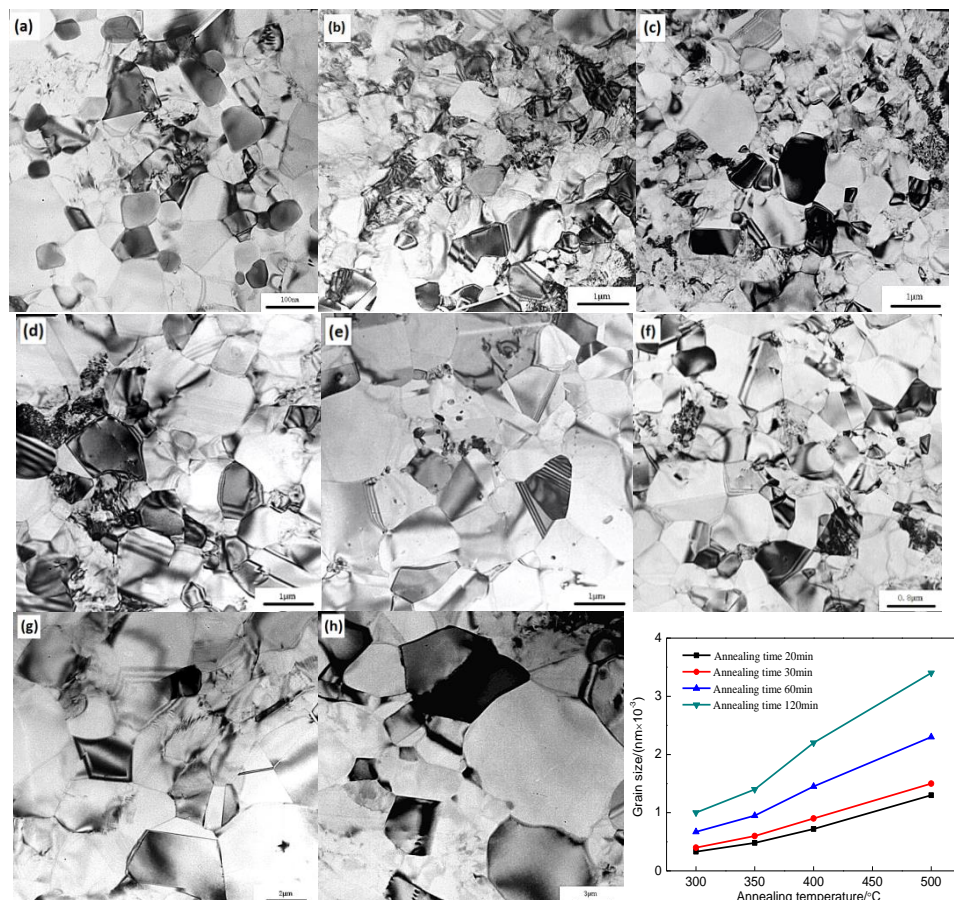


Figure 2. Tensile stress-strain curves of tested steels with different annealing temperatures.

Figure 2 shows the stress-strain curve of ultrafine-grained stainless steel annealed at different temperature and soaked 30 min. As shown in figure 2, the stress-strain curves of tested steel are continuous yield under different annealing temperatures, and there is no obvious yield platform. The change regularity of their strength and elongation is that the tensile strength and yield strength decrease gradually with the increase of annealing temperature, while the elongation increases gradually. Compared with the stress-strain curves of tested steel at different annealing time, the curve of tested steel is more dispersed at different annealing temperatures. This indicates that the mechanical property of tested steel is more sensitive to the temperature change than soaked time in the low temperature annealing process.

### 3.2. Microstructure characterization

Figure 3 shows the microstructure of tested steels with different annealing processes obtained from the TEM images. It can be seen that the microstructure of initial stainless steel was mainly made of fine polygon austenite structure, and the boundary of that was clear as illustrated in figure 3(a). There are low dislocation density and some high angle boundaries in the austenite, due to the contrast image of adjacent grains in TEM image. The average grain size of initial stainless steel microstructure is  $(100\pm 20)$  nm measured by Image Pro Plus. At this size level of the grain, the tested steel exhibited "the brittle fracture behavior" during the uniaxial tension test. It is because when the grain size is very small, the number of grain boundaries increases significantly. Moreover, the simultaneous slip probability of grain boundaries in the same direction may decrease, so the mobility of grain boundaries will be weakened. Due to the decreasing of grain diameter, the removable distance of dislocation is decreasing, which may limit the mobility of dislocation. Therefore, the pinning effect of grain boundary on dislocation is enhanced [14,19]. Figures 3(b)-3(e) show the microstructure of tested steels annealed at 300°C, 350°C, 400°C and 500°C respectively, and soaked 30 min. There was no obvious change in the microstructure and phase constituents of tested steels, but the grain size of them obviously increased. The effective average grain size is respectively  $(0.4\pm 0.03)$   $\mu\text{m}$ ,  $(0.6\pm 0.03)$   $\mu\text{m}$ ,  $(0.9\pm 0.03)$   $\mu\text{m}$  and  $(1.5\pm 0.03)$   $\mu\text{m}$  measured by Image Pro Plus. A few dislocation lines and dislocation tangle can be observed near the grain boundary. Simultaneously, the grain boundary in local area became blurred and a small amount of annealing twins appeared. This illustrates that the grain boundary migration and grain growth occurred in low temperature annealing process.



**Figure 3** TEM image and grain size of the tested steel with different annealing process: (a) Original steel; (b) 300°C +30 min; (c) 350°C +30 min; (d) 400°C +30 min; (e)500°C +30 min; (f)400°C +20 min; (g) 400°C +60 min; (h) 400°C +120 min.

Figures 3(f)-3(h) show the microstructure of tested steels annealed at 400°C and soaked 20 min, 30 min, 60 min and 120 min. Their effective average grain size are respectively  $(0.7\pm 0.03)$   $\mu\text{m}$ ,  $(0.9\pm 0.03)$   $\mu\text{m}$ ,  $(1.3\pm 0.03)$   $\mu\text{m}$  and  $(2.2\pm 0.03)$   $\mu\text{m}$ . It can be seen from the statistical results of effective average grain size, the change of grain size is more sensitive to the change of annealing temperature. After annealing treatment, the strength of tested steel decreased with the increase of grain size, and the yield strength metted the Hall-Petch relationship. Moreover, the plasticity of tested steel significantly increased, and this is in accordance with the results of the literature [14,16-19]. It indicates that the strengthening and toughening mechanism of classic fine grain strengthening will no longer be applied to ultrafine grain materials, so it is necessary to reveal the strength and plastic mechanism of ultrafine-grained materials in the micro level of grain boundary and dislocation.

### 3.3. Internal friction-temperature spectrum

Figure 4(a) shows the internal friction spectrum of tested steel annealed at 400°C with different annealing time. The background internal friction was deducted from internal friction-temperature spectrum as shown in figure 4(b), so it can be seen that the actual  $P_1$  peak increased first and then decreased with the extension of tempering time. When the annealing times were 60 min and 120 min, the values of  $P_1$  peak were maximum and minimum, respectively. According to the calculated internal friction peak activation energy and characteristic parameters [20-22],  $P_1$  peak is the Snoek peak which is caused by the interaction between solid solution atoms and dislocation. In the initial stage of annealing, solid solution atoms migrated to the dislocations, so the concentration of it gradually increased near dislocations. The continuous diffusion of solid solution atoms in this process would lead to the enhancement of relaxation phenomenon of  $P_1$  peak. When the segregation of solid solution was saturated, the value of  $P_1$  peak was maximum. With the extension of tempering time, the pinning effect of a large number of solid solution atoms on the dislocation began to appear, so the interaction between the solid solution atoms and dislocations was enhanced to result in the decrease of  $P_1$  peak value. Figure 4(c) is the actual curve of  $P_2$  peak, the peak height change of it is different from the  $P_1$  peak. It was shown that the  $P_2$  peak height decreased first and then increased with the extension of tempering time. It is because that  $P_2$  peak is the SKK peak which is caused by the common interaction between dislocations, or dislocation and precipitated carbide [23,24]. When the solid solution atoms began to saturate at the position of dislocations, the second phase would precipitate to pin the dislocations. It resulted in the decrease of the  $P_2$  peak height. With the extension of annealing time, the pinning effect weakened due to the second phase precipitation coarsening, and the interaction between dislocations would play a leading role at this time. It led to the rise of  $P_2$  peak height. The  $P_3$  peak is Kê peak which is caused by the interaction of grain boundary structure, grain boundary area and grain boundary movement [25]. With prolonging annealing time, the grain size of tested steel constantly increased, and the number of grain boundaries decreased. So the  $P_3$  peak height had reduced at all times as illustrated in figure 4(d). It can be shown from figure 4 that the peak temperature of  $P_1$ ,  $P_2$  and  $P_3$  peak moved right with the prolonging annealing time, except for the peak temperature of  $P_2$  peak left shift with annealing 120 min.

Figure 5 shows the free attenuation internal friction curve of tested steel annealed 60 min at different temperature. Each internal friction curve has three internal friction peaks (the  $P_1$ ,  $P_2$  and  $P_3$  peak), and the curves of  $P_1$ ,  $P_2$  and  $P_3$  peak at different temperatures were obtained after deducting the background as shown in figures 5(b)-5(d). As shown in figure 5(b), at first the higher the annealing temperature is, the higher the value of  $P_1$  peak height is. It is because that the annealing temperature is higher, solid solution atoms may get more thermal excitation energy. The time used for the aggregation of solid solution atoms near dislocations is shorter. Thus it will cause the effect of solid solution atoms on the dislocation mobility to take place earlier. When the annealing temperature is more than 400°C, the value of  $P_1$  peak height begins to decrease. The reason is due to the reduction of dislocation density or the excessive concentration of solid solution atoms near the dislocations, the pinning effect on the dislocation may increase, which reduces the mobility of dislocations. The curve of  $P_2$  peak height first decreases and later increases with the increase of annealing temperature as

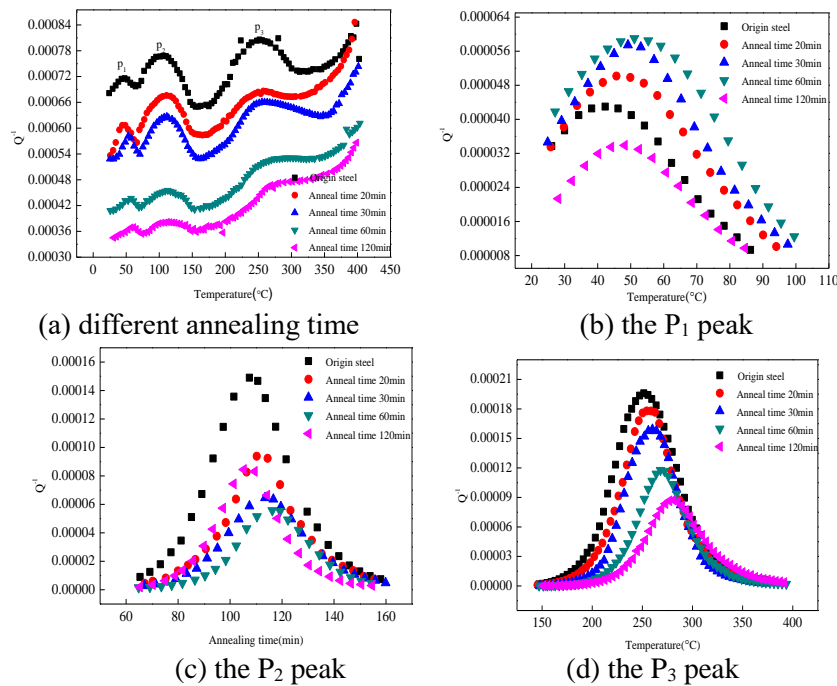


Figure 4. The curves of free damping internal friction with different annealing time.

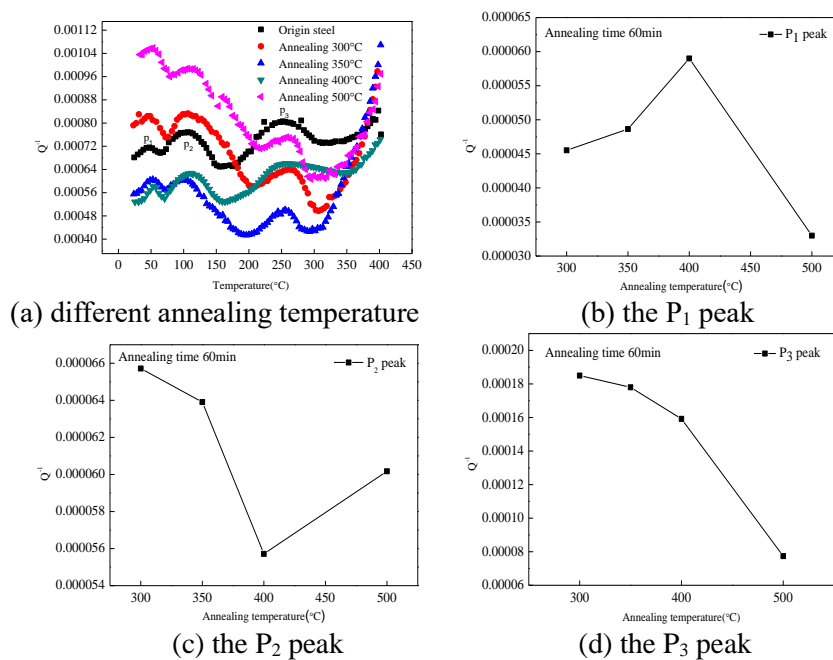


Figure 5. The curves of free damping internal friction at different annealing temperature.

shown in figure 5(c), when the peak value reached the minimum at 400°C. That is because that the carbide which pinned dislocation movement precipitated faster with the higher annealing temperature. As annealing the temperature continues to rise, it may miss the optimum temperature of carbide precipitation "tip temperature". So the carbide precipitation slows down, the carbides begin coarsening, which results in the pinning force on dislocations decrease. It can be seen from figure 5(d) that the

curve of  $P_3$  peak height assumes first slow decreasing and then drastic declining with the increase of annealing temperature.

In order to investigate the internal friction caused by grain boundary relaxation more accurately, the  $P_3$  peak of tested steel under different grain sizes was measured by forced vibration method. The vibration frequencies were 1 Hz, 2 Hz, 4 Hz and 6 Hz, respectively. Figure 6 is the internal friction curve of tested steels whose average grain size is respectively 100 nm, 400 nm, 600 nm, 1300 nm and 2800 nm at 2 Hz vibration frequency. Peak temperature of the internal friction curve is 604.96°C, 612.96°C, 616.06°C, 626.58°C and 641.26°C, respectively. Using transform frequency method and Arrhenius formula [26] to calculate the activation energy of internal friction peak:

$$\tau = \tau_0 e^{H/(k_B T)} \quad (2)$$

where,  $\tau$  is relaxation time;  $\tau_0$  is pre exponential factor.

The calculated activation energies are respectively 197.18 kJ/mol, 201.03 kJ/mol, 207.76 kJ/mol, 219.30 kJ/mol and 231.81 kJ/mol. It can be seen from figure 6(a) that the starting temperature which internal friction peak began to rise was determined by the grain size of tested steel. For tested steel with 100 nm grade internal friction peak, the starting temperature was nearly 100°C lower than that of 2800 nm grade tested steel. This is because that the activation energy of internal friction peak increases with the increase of grain size. When the grain size of tested steel is 2800 nm, it needs higher temperature to meet the demand of larger activation energy. Moreover, the peak height of internal friction peak decreases with the increase of grain size, and that of 2800 nm grade tested steel decreases sharply. It is because that the grain size level has exceeded the scope of ultrafine grain steel. Overall, about the internal friction caused by grain boundary sliding, the grain size is smaller, the activation energy at the beginning of relaxation is smaller, and the distance of grain boundary movement is shorter.

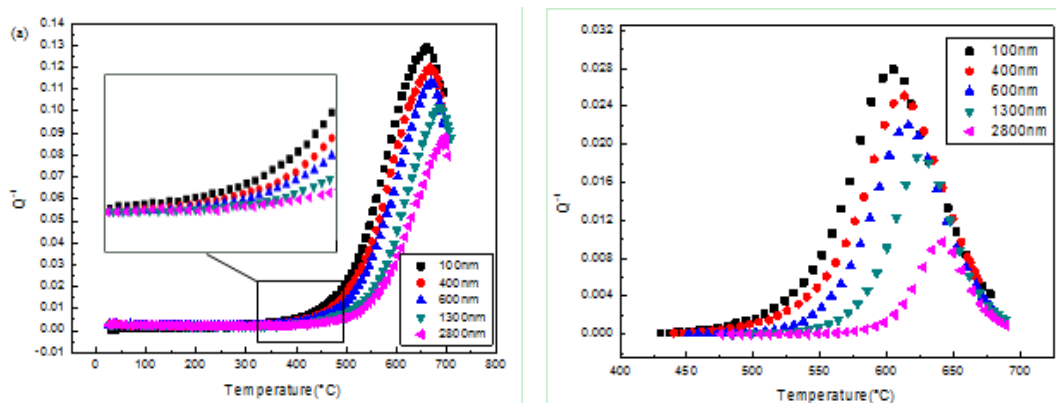


**Figure 6.** The curves of free damping internal friction with different grain size: (a) the curves of forced vibration internal friction; (b) the  $P_3$  peak.

#### 4. Analysis and discussion

The strength and plasticity of metal materials is mainly affected by dislocation movement. When the solid solution atom, the second phase or the grain boundary pins the dislocation to make it impossible to move freely, the macroscopic mechanical properties reflected by this micro-mechanism of interaction is the strength increase of material. Conversely, the dislocation is easier to move, and the plasticity of material is better [26-28]. The strength and plasticity mechanism of ultrafine-grained stainless steel in this paper are as follows: with the increase of grain size, the tensile and yield strength decreases, and the elongation increases gradually as shown in figures 1 and 2. It seems to be contrary to the classic "fine-grained strengthening mechanism" for ultrafine grained metals. Due to a substantial increase in the number of grain boundary, the interaction between dislocations and dislocation, or

grain boundary and dislocation, or the movement of dislocation and grain boundary will produce different synergy mechanism.

Figures 4(b) and 5(b) shows the peak height of  $P_1$  peak first increases and then decreases with the increase of annealing time and annealing temperature. In essence, different annealing processes change the grain size of tested steel, when the grain size is less than 900 nm, with the increase of grain size, the migration distance of solid solution atom to dislocation may increase. It leads to an increase in the peak height of  $P_1$  peak. When the grain size reaches a critical value between 900~1300 nm, the migration of solid solution atom to dislocation will reach critical value, and the peak height no longer increases with the increase of the grain size. At this time, the segregation of solid solution atom plays a leading role in the dislocation pinning, and the mobility of dislocation became weakened. This leads to the decrease of  $P_1$  peak height. The peak height of  $P_2$  peak first decreases and then increases with the increase of annealing time and annealing temperature as shown in figures 4(c) and 5(c). It indicates that when the grain size is less than 900 nm, the number of dislocation and carbides in the unit grain may increase with the increase of grain size. The interaction between dislocation and dislocation may increase, which leads to the decrease of  $P_2$  peak height. However, when the grain size is larger than 900 nm, the movement distance of dislocation increases with the increase of grain size. Due to the coarsening of the second phase carbide, the effect of pinning dislocation is weakened, which led to the  $P_2$  peak height rising. For the internal friction ( $P_3$  peak) caused by the grain boundary relaxation, the peak height decreases with the increase of grain size, and the peak temperature shifts to the right as shown in figures 4(d) and 5(d). There are two main factors affecting the grain boundary relaxation [25]: One factor is the boundary itself, including the geometry configuration of grain boundary, such as the Orientation and mismatch relation on both sides of grain boundary. The other factor is external factors, such as the adsorption of impurities, etc. All of these may affect the mobility of grain boundary. Mori T's research [29] shows the relaxation time of grain boundary increases with the increase of grain size, that means, the distance of grain boundary sliding in the relaxation time increases with the increase of grain diameter. This is in accordance with the regularity shown in figure 6, the critical temperature when the internal friction of grain boundary begins to increase rapidly increases with the increase of grain size. Therefore the larger the grain size, the greater the activation energy required for grain boundary sliding, namely, the greater the sliding resistance.

According to present study the strength and plasticity mechanism of ultrafine-grained stainless steel does not only depend on the interaction between dislocations, but also the interaction between grain boundary and dislocation might effect as well. When the grain size is below 900 nm, the dislocation and grain boundary are easy to be pinned and hard to move. The strength of material is high and the plasticity is poor. As the grain is coarsening (more than a critical size within 900~1300 nm), although the resistance of grain boundary sliding increases, the increase of the grain boundary number and grain diameter may lead to the weakening of pinning effect on dislocation. In addition, the distance of grain boundary sliding increases with the increase of grain diameter, these make the movement of grain boundary become enhanced. So the strength of material decreases and the plasticity increases.

## 5. Conclusions

With the increase of annealing temperature and annealing time, the tensile strength and yield strength of tested steel decrease, and the elongation of tested steel increases gradually. Moreover, the mechanical property of tested steel is more sensitive to the temperature change than soaked time in the low temperature annealing process. In order to obtain better plasticity in stainless steels 400°C and 60 min annealing is recommended. The  $P_1$  peak of tested steel first rises and then decreases, the  $P_2$  peak first decreases and then increases, and the  $P_3$  peak decreases constantly. In essence, the strength and plasticity mechanism of ultrafine-grained stainless steel is not only the interaction between dislocations, but also the interaction between grain boundary and dislocation should be considered.

## Acknowledgments

Supported by National Nature Science Foundation of China (No. 51274121); Supported by State Key

Laboratory of Marine Equipment made of Metal Material and Application (No. SKLMEA-USTL-201708); National Nature Science Foundation of USTL (No. 2017QN11).

## References

- [1] Yin Y Q, Wu C L, Xie P, Zhu K, Tian S L, Han M and Chen J H 2016 *J. Acta Metall. Sin.* **12** 1527-35
- [2] Yang G, Liu Z D, Gong Z H, Wang L M, Lin Z J and Cheng S C 2006 *J. Iron steel Res.* **18** 32-6
- [3] Muley S V, Vidvans A N, Chaudhari G P and Udainiya S 2016 *Acta Biomater* **30** 408-19
- [4] Tang L L, Zhao Y H, Islamgaliev R K, Chi Y A, Valiev R Z, Lavernia E J and Zhu Y T 2016 *KnE. Mater. Sci.* **1** 168-71
- [5] Song Y P, Chen M M, Gao D S and Wang W 2017 *J Hot Working Technol.* **3** 6-9
- [6] Zhang Q, Liu Y, Liu Y S, Ren Y H, Wu Y X, Gao Z P, Wu X L and Han P D 2017 *J. Mater Sci Eng. A* **701** 196-202
- [7] Wang Q, Mu Y, Lin J, Zhang L and Roven H J 2017 *J. Mater. Sci. Eng.* **699** 26-30
- [8] Wang X 2013 Research on mechanical properties of ultra-fine grain AZ31 magnesium alloy prepared by powder metallurgy (Harbin: Harbin Institute of Technology)
- [9] Qian T, Karaman I and Marx M 2014 *Adv. Eng. Mater.* **16** 1323-39
- [10] Morris D G, Gutierrez-Urrutia I and Muñoz-Morris M A 2008 *J Mater. Sci.* **43** 7438-44
- [11] Lan H, Liu W J and Liu X 2008 *Chin. J. Mater. Res.* **22** 279-86
- [12] Etienne A, Radiguet B, Genevois C, Breton J M, Valiev R and Pareige P 2010 *Mater. Sci. Eng.* **527** 5805-10
- [13] Park K T, Kim Y S, Lee J G and Dong H S 2000 *Mater. Sci. Eng.* **293** 165-72
- [14] Xu D M, Li G Q, Wan X L, Xiong R L, Xu G, Wu K M, Somani M C and Misra R D K 2017 *Mater. Sci. Eng. A* **688** 407-15
- [15] Ebrahimi F and Li H 2007 *J Mater Sci.* **42** 1444-54
- [16] Zheng Z G, Xie C J, Sun T and Yuan S 2014 *Mater. Mech. Eng.* **50** 77-83
- [17] Rodríguez-Baracaldo R, Benito J A and Cabrera J M 2010 *J. Mater. Sci.* **4517** 4796-804
- [18] Gao S, Chen M, Joshi M, Shibata A and Tsuji N 2014 *J. Mater. Sci.* **49** 6536-42
- [19] Haddad M, Ivanisenko Y, Courtois-Manara E and Fecht H J 2015 *Mater. Sci. Eng.* **620** 30-5
- [20] Li W J, Zhang H Y, Fu H, Zhang J and Qi X Y 2015 *Acta Metall Sin.* **51** 385-92
- [21] Wang H, Li W, Hao T, Jiang W B, Fang Q F, Wang X P, Zhang T, Zhang J, Wang K and Wang L 2017 *Mater. Sci. Eng.* **695** 193-8
- [22] Zeng B, Wu J, Shen B and Zhang H 2011 *Shanghai Met.* **33** 18-21
- [23] Ge T S and Wang Q M 1955 *Acta Phys. Sin-Ch Ed.* **11** 387-402
- [24] Xu L Y, Ji J, Huang J, Zhu Z H, Wu Y W and Wang H B 2016 *Phys Testing Chem. Anal. Part A* **52** 156-8
- [25] Ge T S 2014 *Solid Internal Friction Theoretical Basis* (Beijing: Science Press) pp 375-425
- [26] Shi D K 1988 *Dislocation and Material Strength* (Xi'an: Xi'an jiaotong univ Press) pp 253-70
- [27] Yu M H 2011 *New System of Strength Theory* (Xi'an: Xi'an jiaotong univ Press) pp 62-83
- [28] Hussein A M, Rao S I, Uchic M D, Parthasarathay T A and Ei-awady J A 2017 *J. Mech. Phys. Solids* **99** 146-62
- [29] Mori T, Koda M, Monzen R and Mura T 1983 *Acta Metall.* **31** 275-83